Journal of the Marine Biological Association of the United Kingdom, 2013, 93(8), 2145–2154.
doi:10.1017/S0025315413000696

Proposed function of alternative oxidase in mitochondrial sulphide oxidation detoxification in the Echiuran worm, *Urechis unicinctus*

JIAN HUANG*, LITAO ZHANG*, JINLONG LI, XIAOLI SHI AND ZHIFENG ZHANG

Key Laboratory of Marine Genetics and Breeding (Ocean University of China), Ministry of Education, Qingdao 266003, China

Alternative oxidase (AOX), a ubiquinol oxidase, introduces a branch pathway to the respiratory electron transport chain (ETC), bypassing complexes III and IV and catalysing the cyanide-resistant reduction of oxygen to water without translocation of protons across the inner mitochondrial membrane. Thus, it functions as a non-energy-conserving member of respiratory ETC. Previous studies of AOX focused on plants and some fungi, whereas data on animals are limited. In this study, full-length AOX cDNA was cloned from the Echiuran worm, Urechis unicinctus*, a marine benthic invertebrate. In addition, mRNA expression pattern of combined activity of cytochrome c oxidase (CCO) in the body wall and hindgut of the worm exposed in sulphide (50 μM and 150 μM) was measured. The results revealed that AOX mRNA expression increased in a time- and concentration-dependent manner in both tissues, was significantly increased at 48 h, and continuously increased with time. In contrast, the activity of CCO decreased significantly at 24 h and was inhibited at 48 h during exposure to 150 μM sulphide. The present data indicate the expression of AOX mRNA depended on the sulphide concentration present as well as being influenced by the physical condition of the worm, especially the CCO activity.*

Keywords: alternative oxidase, cytochrome *c* oxidase, sulphide, *Urechis unicinctus*

Submitted 1 May 2012; accepted 7 May 2013; first published online 22 July 2013

INTRODUCTION

Sulphide, which usually refers to three forms of hydrogen sulphide—hydrogen sulphide gas (H_2S), the bisulphide anion (HS^-) and the sulphide anion ($S2^-$) (Millero *et al.*, 1988)—is a well-known toxin that inhibits many enzymes involved in aerobic metabolism, such as cytochrome *c* oxidase (CCO), a mitochondrial terminal oxidase. The CCO causes harm to organisms, including sulphhaemoglobin formation (Affonso *et al.*, 2004; Bailly & Vinogradov, 2005), mitochondrial depolarization (Eghbal *et al.*, 2004) and increased free radical production by inducing reactive oxygen species (ROS) leading to oxidative stress (Affonso & Rantin, 2005; Attene-Ramos *et al.*, 2007). Nevertheless, a variety of marine invertebrates living in habitats such as hydrothermal vents, hydrocarbon seeps, coastal mudflats and marshes that periodically encounter or are continuously exposed to sulphide can survive (Bagarinao, 1992; Goffredi *et al.*, 1997; Julian *et al.*, 1999; Buchner *et al.*, 2001; Joyner-Matos *et al.*, 2010).

The capability of animals to tolerate sulphide is thought to result from specialized sulphide oxidation detoxification mechanisms, such as mitochondrial sulphide oxidation, which reduces the toxicity of thiosulphate (Grieshaber & Völkel, 1998). Some invertebrates such as the gutless clam *Solemya reidi* (Powell & Somero, 1986; Kraus *et al.*, 1996) and the lugworm *Arenicola marina* (Hildebrandt & Grieshaber, 2008a; Theissen & Martin, 2008) can oxidize sulphide in their mitochondria. The first step in mitochondrial sulphide oxidation is presumably catalysed by a mitochondrial membrane flavoprotein, sulphide: quinone oxidoreductase (SQR), which oxidizes sulphide to persulphide. The sequential actions of a sulphur dioxygenase and a sulphur transferase (or rhodanese) are proposed to convert SQR-bound persulphide into sulphite and thiosulphate, respectively. Finally, the product of the sulphur dioxygenase reaction, sulphite, can be directly oxidized to sulphate by sulphite oxidase and alternatively converted by sulphur transferase to thiosulphate (Hildebrandt & Grieshaber, 2008b; Taniguchi *et al.*, 2009; Tiranti *et al.*, 2009; Kabil & Banerjee, 2010; Ma *et al.*, 2010) (Figure 1).

Eukaryotic anaerobes containing the same basic set of genes and enzymes for anaerobic energy metabolism and alternative oxidase (AOX) in mitochondria may help to maintain redox balance (Muller *et al.*, 2012). In addition, the same low glycolytic rate was observed in mitochondria or eukaryotic anaerobes during either anoxia or sulphide stress (Oeschger & Storey, 1990). Anoxia and sulphide could be inhibited CCO. In marine invertebrates, AOX also maintains respiratory electron flux, substrate oxidation and cellular redox potential when CCO is inhibited (Abele *et al.*, 2007). High concentrations of sulphide can bind reversely at the haeme site of cytochrome aa_3 (Nicholls, 1975), to inhibit the transfer of electrons from

*Joint first authors

Corresponding author:
Z. Zhang
Email: zzfp107@ouc.edu.cn

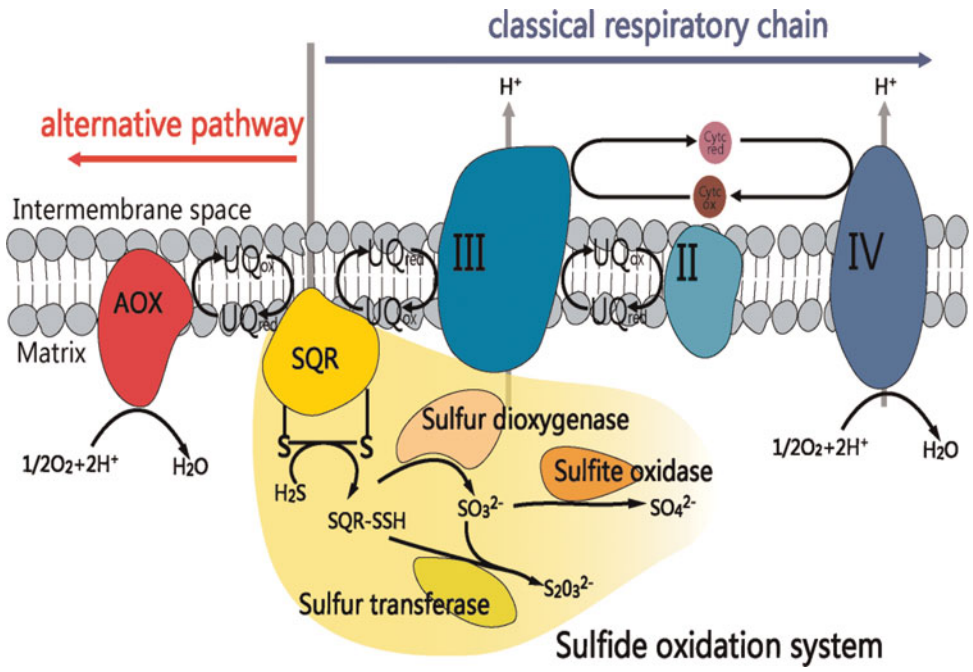

Fig. 1. The proposed model of two different pathways for sulphide oxidation in the mitochondria (modification from Kabil & Banerjee, 2010). Electrons from the sulfide oxidation system can be transferred to oxygen either by the alternative pathway or the classical respiratory chain. The enzymes, complexes and respective substrates in relation to the inner mitochondrial membrane are depicted in the schematic drawing. II, complex II (succinate: ubiquinone oxidoreductase); III, complex III (ubiquinol: cytochrome *c* oxidoreductase); IV, complex IV, (cytochrome *c* oxidase); AOX, alternative oxidase; SQR, sulphide: quinol oxidoreductase; UQ, ubiquinone pool.

sulphide oxidation via CCO. In this case, electrons are transferred to oxygen by another pathway, the alternative mitochondrial respiratory pathway (Figure 1). This pathway branches at the ubiquinone pool and consists of AOX, which presumably resembles the enzyme found in plant mitochondria and has a central role in cyanide-resistant respiration, as well as acting as an alternative terminal oxidase in the electron transport chain (ETC). It catalyses the oxidation of ubiquinol, reducing molecular oxygen to water, without translocation of protons across the inner mitochondrial membrane. The redox energy that is not conserved for ATP synthesis is released as heat (Vanlerberghe & McIntosh, 1997).

Recently, AOX studies have focused on plants and microbes. The structure of the plant AOX model has been determined and all plant AOX amino acid sequences (in the C-terminal domain) contain two copies of the conserved iron-binding motif (E-X-X-H). Three fully conserved residues (T, E, Y) in the pocket were thought to be potential ligands for ubiquinone (Sluse & Jarmuszkiewicz, 1998). However, limited data have been reported for AOX in animals. Nucleic acid sequences similar to plant AOX have been identified in some invertebrates, such as the chordate *Ciona intestinalis* Linnaeus and the oyster *Crassostrea gigas*. The AOX of *Ciona intestinalis* was first expressed in human kidney cells (Hakkaart *et al.*, 2006) and then *Drosophila melanogaster* cells (Fernandez-Ayala *et al.*, 2009), based on cDNA sequences from *C. intestinalis* genomic data. The oyster, *Crassostrea gigas*, AOX sequence was recently cloned (McDonald *et al.*, 2009). In permeabilized fibres from the sandworm *Nereis (Neanthes) virens*, AOX activity could be triggered both by the redox state of the cell and the type of substrates provided to mitochondria (Pichaud *et al.*, 2012).

Owing to its character, AOX may allow animals to acclimate to stressful conditions, particularly those that inhibit the cytochrome pathway. Biochemical studies in *A. marina* demonstrated rapid mitochondrial sulphide detoxification via the AOX pathway that was regulated by the redox state of the organism (Hildebrandt & Grieshaber, 2008a).

In the present study, full-length cDNA of AOX was cloned from the Echiuran worm *Urechis unicinctus*, mainly present in China, Korea, Russia and Japan, and inhabiting marine coastal sediments. In addition, we measured AOX mRNA expression patterns coupled with the activity of CCO in the body wall and hindgut of the worm during sulphide exposure. Our aim was to determine the AOX expression characteristics during sulphide exposure, and extend our understanding of the regulation of mitochondria sulphide detoxification in animals.

MATERIALS AND METHODS

Animals and experimental design

Urechis unicinctus, collected from a coastal intertidal flat in Yantai, China, were non-damaged and of a homogeneous size (20 ± 2 cm body length). The worms were maintained for one week in an aerated, circulating seawater aquarium (20 ± 1°C, pH 7.8 ± 0.1, salinity 28‰) and fed with microalgae (*Chlorella vulgaris* and *Mtzschia closterium*). Feeding was stopped 24 h before the experiment.

The concentration of sulphide treatment was defined as 50 and 150 μM by diluting a stock sulphide solution (10 mM Na_2S, pH 8.0). Natural seawater was used as a control. Each group contained three replication tanks. Each tank (60 × 40 × 40 cm) contained 15 worms with 30 l seawater. The continuous sulphide concentration was maintained by adding the stock solution every 2 h based on a previous examination for measuring the change of sulphide concentration in each tank.

https://doi.org/10.1017/S0025315413000696 Published online by Cambridge University Press

Two worms were sampled from each tank (i.e. four individuals from each group) at 0, 6, 12, 24, 48 and 72 h after initiation of sulphide exposure. The body wall and hindgut of the worms were excised, frozen in liquid nitrogen, and stored at −80°C for subsequent analysis.

RNA isolation and cloning of full-length cDNA

Total RNA was extracted from the body wall and hindgut tissues using Trizol (Invitrogen), according to the manufacturer's instructions. All RNA isolations exhibited an A260/A280 >1.5. First-strand cDNA was synthesized using a reverse transcription system (Takara).

To obtain an AOX cDNA fragment, nested degenerate primers were designed based on evolutionarily conserved domains from known AOX sequences available at the National Center for Biotechnology Information (NCBI). The primary degenerated primers were: Forward 5′-ARGCNGA RAAYGARMGNATGCA-3′ and Reverse: 5′-GCYTCYTCYT CNARRTANCC-3′; pair of nest primers were: N_1 5′-GAYY AYGGNTGGATHCAYAC-3′ and N_2: 5′- CKRTGRTGIGC YTCRTCNGC-3′. The obtained fragment was sequenced by an ABI PRISM 3730 DNA sequencer. Sequence alignment by Blastx from NCBI was performed using the DNA fragment, and demonstrated 75% identity to *Crassostrea virginica* AOX sequence. Thus, the fragment was preliminarily confirmed as part of an AOX sequence.

The full-length cDNA of AOX was obtained using 5′- and 3′-rapid amplification of the cDNA ends (RACE) PCR technique performed by the SMARTer™ RACE cDNA Amplification kit (Clontech). The 5′- and 3′-RACE-Ready cDNAs were prepared according to the manufacturer's instructions. Two gene-specific primers (GSP), GSP-5′ 5′-AGGTATCCCACAAAACGATGGCAGAG-3′ and GSP-3′ 5′-AGAACGAGCGTATGCACCTGATGGT-3′ were designed to clone the 5′ and 3′ ends of AOX cDNA, respectively. The RACE PCR reactions were performed by Advantage II Polymerase Mix (Clontech). The 3′- and 5′-RACE products were sequenced and assembled.

Sequence analyses

Sequence similarity search for nucleotides and amino acids used the BLAST program from the NCBI (http://www.ncbi.nlm.nih.gov/BLAST/). The subcellular location of proteins was predicted with TargetP (http://www.cbs.dtu.dk/services/TargetP) and the transmembrane region was determined by TMHMM-2.0 (http://www.cbs.dtu.dk/services/TMHMM-2.0). Multiple sequence alignments of AOX proteins were generated using the Clustal X program. The phylogenetic tree was computed and constructed using MEGA 4.0 with the neighbour-joining method using the Poisson correction amino acid substitution model and the complete deletion gaps option. Bootstrap values from 1000 replicates were calculated and indicated at branch points on the neighbour-joining tree.

Analysis of relative AOX gene expression in tissues

Body wall and hindgut RNA isolation and cDNA synthesis were achieved as described above. The synthesized cDNA was diluted (1:100) for real-time RT-PCR. Relative quantifications of AOX mRNA expression were performed in duplicate, at least, for every sample. Real-time RT-PCR was performed using a fluorescence temperature cycler (7500 Real-Time PCR Systems, Applied Biosystems, Foster City, USA) in the presence of SYBR-green. The optimized reactions of real-time RT-RCR were conducted according to the manufacturer's instructions (Takara SYBR Premix Ex Taq) using *U. unicinctus β-actin* (GenBank Accession No. GU592178.1) as an internal standard. The primer sequences were as follows: AOX-F 5′-GTAGCCTTGCCTCATCCCATC-3′, AOX-R 5′-TTCATCTTGTCTCCCTCTGCTG-3 giving a product of 165 base pairs (bp); *β-actin*-F 5′-CACACTGTCC CCATCTACGAGG-3′, *β-actin*-R 5′-GTCACGGACGATTA CACGCTC-3′ generating a product of 153 bp. Data were analysed using the 7500 System Sequence Detection Software (Applied Biosystems) with the $2^{-\Delta\Delta Ct}$ method.

Isolation of mitochondria and cytochrome *c* oxidase (CCO) activity assay

The isolation of mitochondria was performed according to the protocol of Schroff (Schroff, 1977). Each sample (400 mg) was homogenized in a glass homogenizer with 9 × volume of pre-cold isolation solution (58.4 mM sucrose, 140.2 mM glycin, 40 mM Tris, 2 mM EGTA, 0.2% bovine serum albumin, pH 7.5). The homogenates were centrifuged (×4000 *g*, 15 min at 4°C), and the supernatants were kept and the pellets discarded. The supernatants were then centrifuged (×12,000 *g*, 10 min at 4°C) in isolation buffer and the pellets contained isolated mitochondria, which were suspended for the enzyme assay. Protein levels in the mitochondria extract were determined using the Bradford (1976) method using bovine serum albumin as a standard.

Cytochrome *c* oxidase activity was evaluated by determining the rate of oxidation of reduced cytochrome *c* using methods described by Hand & Somero (1983) with some modification. Briefly, the assay solution contained 0.1 M Tris-HCl (pH 6.0), and 1 ml 0.2% reduced cytochrome *c* (Sigma from equine heart), in a total volume of 2.0 ml. Then, 10 μl mitochondria extract was added and the reaction was measured by recording the decrease in absorbance at 550 nm. One unit of CCO was defined as 0.001 decrease of OD_{550} at 1 min per 1 mg protein (U/mg protein/min). Each sample was detected at least in duplicate.

STATISTICAL ANALYSIS

All data were presented as mean ± standard error (SE). Significant differences between treatments were evaluated using one-way analysis of variance (ANOVA) followed by the Duncan method, and between pairs of data by the Student's *t*-test, using the SPSS statistical package (Version 18.0). Values of $P < 0.05$ were considered statistically significant.

RESULTS

Sequence and analysis

The PCR product amplified by the degenerate primers was 165 bp and its amino acid sequence was significantly

https://doi.org/10.1017/S0025315413000696 Published online by Cambridge University Press

homologous to other known AOXs, with 75% homologous identity to *Crassostrea virginica*. Based on the partial sequence, two fragments of 1091 bp and 791 bp were cloned by 5′- and 3′-RACE, respectively, and assembled to a full-length AOX cDNA of 1725 bp (GenBank Accession No. HQ822262).

The complete sequence of AOX cDNA consisted of a 5′terminal untranslated region (UTR) of 288 bp, a 3′UTR of 390 bp and an open reading frame (ORF) of 1047 bp, which contained a termination codon (TAA) and encoded a putative protein of 348 amino acids (Figure 2) with a molecular mass of 39.49 kDa and a theoretical isoelectric point (pI) of 8.49. The deduced protein contained conserved LET, NERMHL, LLEEA, RADE_ _H regions and a Q-binding site, which are the main characteristics of AOX. TargetP analysis showed that *Urechis unicinctus* AOX was located in the mitochondria, with a score of 0.673. Topology prediction for the 348 amino acid protein by TMHMM demonstrated the protein had two transmembrane helices (TMHelix I 170-192 aa and TMHelix II 233-255 aa, Figure 2).

Sequence analysis by the NCBI BLAST program revealed that the putative amino acid sequence of *U. unicinctus* AOX shared high identity with other AOXs in plants, parasites, green algae, fungi and some metazoans. Alignment of AOX sequences demonstrated they shared well-conserved motifs characteristic of alternative oxidase. Similar to other animal AOXs, *U. unicinctus* AOX possesses a C-terminal motif N-P-Y-[KE]-P-G that is not present in AOX proteins from other kingdoms (Figure 3A). A phylogenetic tree was constructed based on amino acid alignment using the MEGA program and the result indicated that *U. unicinctus* AOX was clustered together with *Capitella* sp., as a sub-cluster of metazoans, while others formed distinct paraphyletic clusters (Figure 3B). Overall, the relationships displayed in the phylogenetic tree were generally in accordance with the taxonomy.

Expression of AOX mRNA and activity of CCO under different sulphide treatments in *Urechis unicinctus* body wall and hindgut

The expression dynamics of *U. unicinctus* AOX mRNA in the body wall and hindgut of worms exposed to different concentrations of sulphide are shown in Figure 4. Distinct dose- and time-dependent elevations of AOX mRNA expression were present in both tissues from the treatment groups during the experiment. In the body wall of worms exposed to 50 μM sulphide, increased AOX mRNA was not significant ($P > 0.05$) during the first 72 h of exposure, while a significant increase ($P < 0.05$) was detected at 72 h and was 16.7-fold higher compared with controls. At 150 μM sulphide, a significant increase ($P < 0.05$) was observed at 48 h after exposure with a 24.1-fold and 40.6-fold increase at 72 h compared with controls, respectively (Figure 4A). In the hindgut, a similar pattern was observed (Figure 4B). However, the timing of the significant increase occurred earlier in the hindgut than in the body wall. In the 50 μM sulphide group, AOX mRNA increased significantly at 48 h with a 17.2-fold higher increase and reached a maximum (52.1-fold higher) at 72 h. In the 150 μM sulphide group, the expression was higher than that of the 50 μM sulphide group except at 48 h (Figure 4B).

The CCO activity, a terminal electron acceptor of classical mitochondrial ETC, increased in the body wall and hindgut of worms at the beginning and then declined during sulphide exposure (Figure 5). At 6 h of sulphide exposure, the CCO activities of both worm tissues exposed to 50 μM sulphide significantly increased ($P < 0.05$), while the increase due to 150 μM sulphide was not significant ($P > 0.05$). The CCO activity decreased significantly ($P < 0.05$) in both worm tissues exposed to 150 μM sulphide for 24 h, and was inhibited (approximately 0) at 48 h. In the 50 μM group, the timing of the significant decrease occurred later than the 150 μM group, which was at 72 h (Figure 5).

DISCUSSION

In this study, the full-length cDNA of AOX from the *Echiuran* worm *Urechis unicinctus* was cloned, and shown to contain a conserved 4-helix bundle, Q-binding site and an animal-specific C-terminal motif. Furthermore, we experimentally demonstrated the expression dynamics of AOX mRNA for the first time, and suggested that alternative pathways exist in the worm by the expression of *U. unicinctus* AOX mRNA and CCO activity when the animal is exposed to sulphide.

Sequence and structure analysis of the alternative oxidase from *Urechis unicinctus*

The currently adopted view is that the active site of AOX comprises a non-haeme di-iron centre, in which the metal atoms are ligated by glutamate and histidine residues within a 4-helix bundle (Gomes *et al.*, 2001). Based on the di-iron centre and assignments of the proposed Glu and His ligands, AOX was predicted to interact with one leaflet of the membrane bi-layer as an integral interfacial membrane protein, referred to as the Andersson and Nordlund (AN) model (Berthold *et al.*, 2000; Moore & Albury, 2008). The model is supported by extensive site-directed mutagenesis studies (Affourtit *et al.*, 2002; Albury *et al.*, 2002), and the presence of a binuclear iron center was later confirmed by electron paramagnetic resonance (EPR) spectroscopy (Berthold *et al.*, 2002; Moore *et al.*, 2008). Using electrochemistry and Fourier transform infrared (FTIR) spectroscopy, the redox properties of recombinant alternative ubiquinol oxidase from the parasite *Trypanosoma brucei* were studied and interpreted in terms of the possible structure of the active site and mechanism of oxygen reduction to water by AOX. This study confirmed the di-iron carboxylate protein model of alternative oxidase (Maréchal *et al.*, 2009). Based on the AN model and bioinformatics, we predicted a schematic structure of *U. unicinctus* AOX in the present study, with four conserved regions ($LE_{179}T$, $NE_{218}RMH_{221}L$, $LE_{269}EEA$, $RADE_{323}AH_{326}$) involved in the formation of the 4-helix bundle, in which the Glu and His residues of the motifs participate in the formation of the bundle required for iron-binding (Figure 6).

To fulfil its main function of transferring electrons to oxygen, a binding site for ubiquinol, the reducing substrate of AOX, must be contained. Albury *et al.* (2010) proposed a model for the ubiquinol-binding site in AOX between helices II and III, leading from a proposed membrane binding domain to the catalytic domain, by bioinformatics analysis and site-directed mutagenesis in plant *Sauromatum*

https://doi.org/10.1017/S0025315413000696 Published online by Cambridge University Press

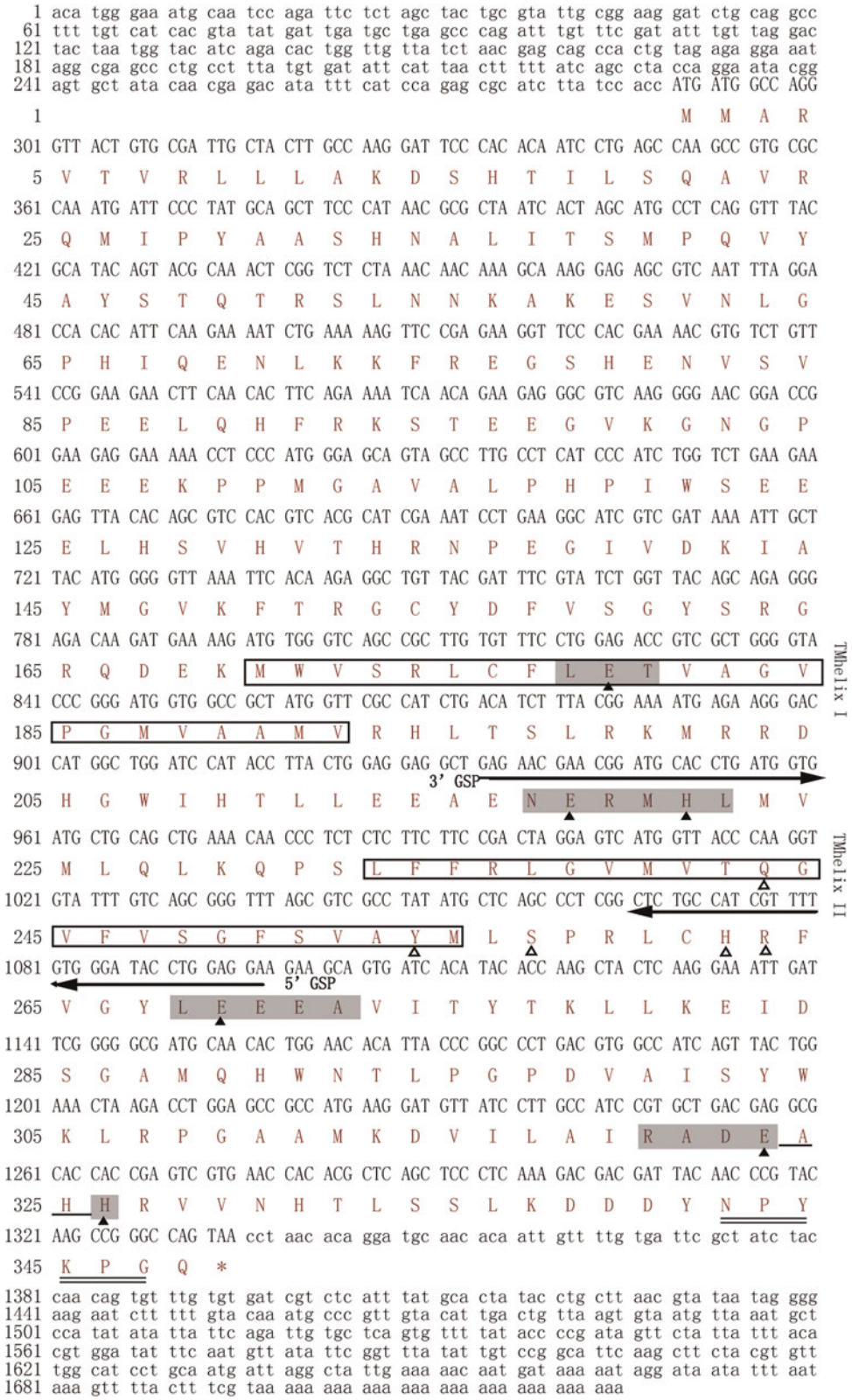

Fig. 2. The full-length cDNA sequence and deduced amino acid sequence of *Urechis unicinctus* AOX. The highly conserved iron-binding motifs are highlighted as shaded regions in which the Glu and His residues are marked by ▲ and the residues for quinol binding are indicated by △. The transmembrane helices (TMhelix) are shown in an open box; RACE gene-specific primers (GSP) are underlined with an arrow; the animal-specific C-terminal motif is demonstrated by double lines.

guttatum AOX expressed in yeast *Schizosaccharmyces pombe*. It was demonstrated that Gln242, Tyr253, Ser256, His261 and Arg262 were critical for ubiquinol-binding (Albury *et al.*, 2010). Multiple sequence alignment of AOX proteins showed that these residues were highly conserved and existed in animals (Figure 3A). Transmembrane prediction of AOX in *U. unicinctus* by TMHMM located the ubiquinol-binding pocket (composed of Gln243, Tyr254, Ser257, His262

https://doi.org/10.1017/S0025315413000696 Published online by Cambridge University Press

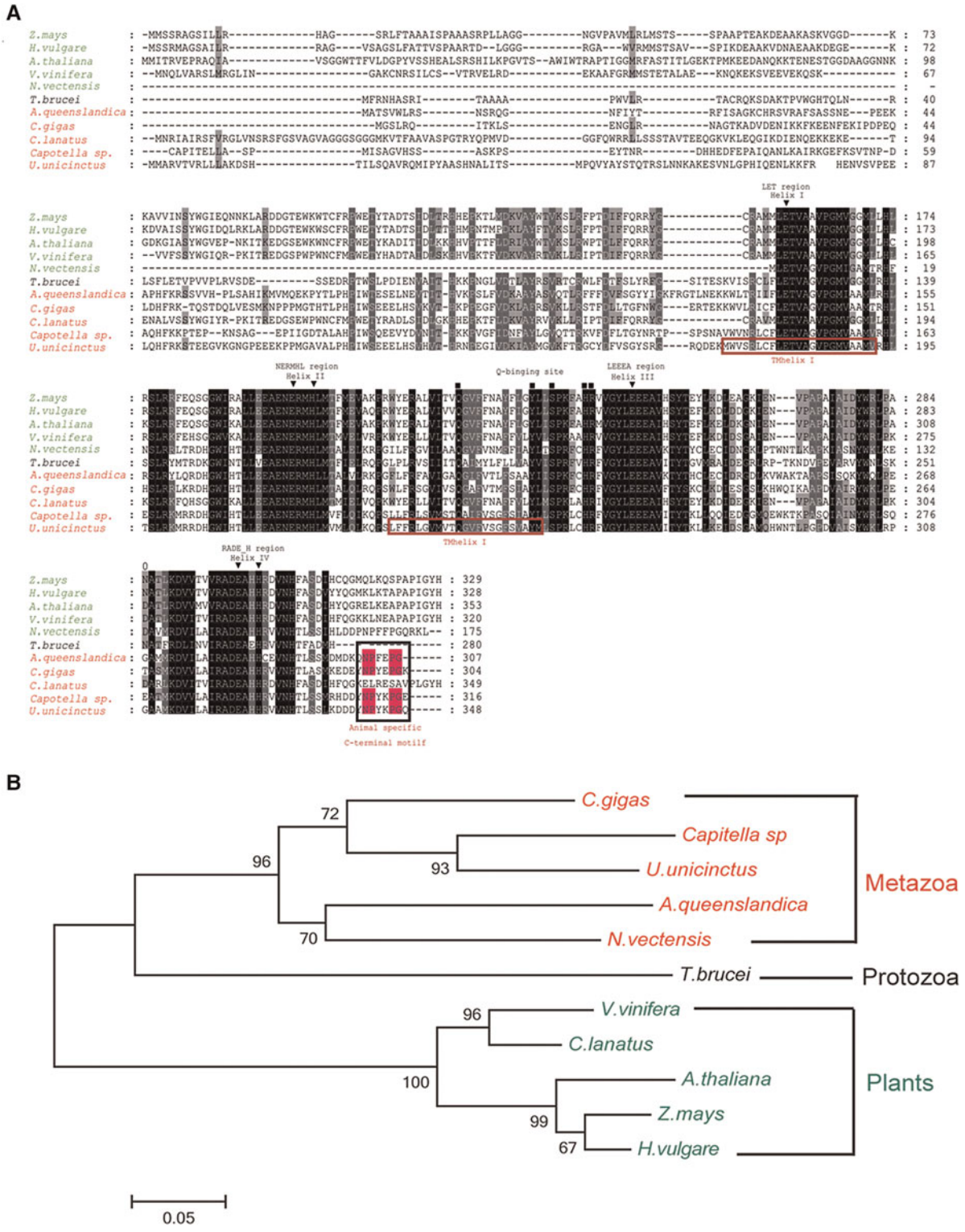

Fig. 3. Sequence comparison of protein encoded by AOX from different species: (A) multiple sequence alignment of AOX sequences from different species. Identical and similar residues are highlighted in black and grey, respectively. Residues for iron-binding and quinol binding are indicated by ▼ and ■, respectively. The transmembrane helices (TMhelix) and the animal-specific C-terminal motif are denoted in the red box; (B) the phylogenetic relationships between AOX from different species constructed by MEGA 4.0 using the neighbour-joining method. The Accession numbers are: *Amphimedon queenslandica* (XP_003385247.1), *Arabidopsis thaliana* (BAB09852.1), *Capitella sp.* (JGI genome), *Citrullus lanatus* (ADD84880.1), *Crassostrea gigas* (EKC33714.1), *Hordeum vulgare* subsp. *Spontaneum* (AEC33278.1), *Nematostella vectensis* (XP_001635929.1), *Trypanosoma brucei brucei* (AAB46424), *Urechis unicinctus* (ADZ36698.1), *Vitis vinifera* (XP_002274470.1) and *Zea mays* (AAB97839). Unless otherwise specified, the sequences were obtained from NCBI. Metazoan species are listed in red, protozoa in black and plants in green. See online publication for colour figure, doi:10.1017/S0025315413000696

and Arg263) in the end of the transmembrane helix (TMhelixII, Figure 2), thus placing the ubiquinol ring near the membrane interface, similar to cytochrome *bo3* ubiquinol oxidase from *Escherichia coli* (Abramson *et al.*, 2000). Such a structure, a transmembrane helix containing Q-binding site followed by a part of the 4-helix bundle (helix III), moved

https://doi.org/10.1017/S0025315413000696 Published online by Cambridge University Press

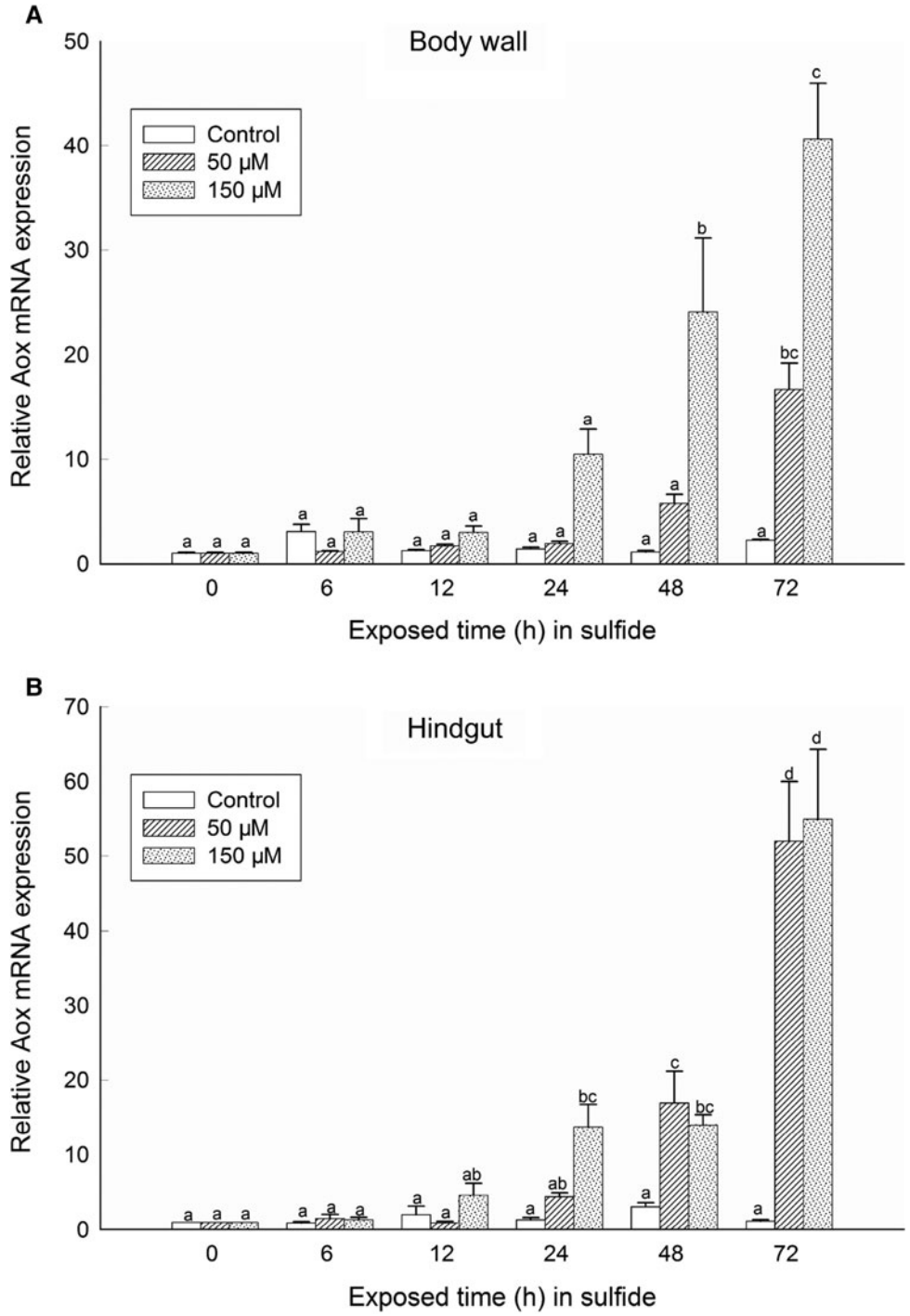

Fig. 4. Relative expressions of AOX mRNA in body wall (A) and hindgut (B) of *Urechis unicinctus* exposed to sulphide. The *β-actin* gene was chosen as a reference gene, and the relative gene expression was analysed according to the $2^{-\Delta\Delta CT}$ method. All data are presented as mean ± SE, $N = 4$ with two replicates. Groups containing the same letters on the bar indicate no significant difference while different letters on the bar indicate significant difference ($P < 0.05$).

the reduced quinol as a substrate of AOX to the di-iron centre and promoted its functions.

Proposed role of AOX in mitochondrial sulphide oxidation detoxification

In the classical respiratory chain of mitochondria, CCO (complex IV) acts as a terminal oxidase to accept electrons from cytochrome *c* and direct them to the four-electron reduction of O_2 with the formation of water and the concomitant translocation of protons across the inner membrane coupled with ATP synthesis (Figure 1). Sulphide can inhibit the activity of CCO by reversibly binding at the haeme site of cytochrome *aa3* (Cooper & Brown, 2008). As ATP synthesis is dependent on the flow of electrons down the electrochemical gradient mediated by enzyme cytochrome complexes, inhibition of any complexes of the respiratory chain

https://doi.org/10.1017/S0025315413000696 Published online by Cambridge University Press

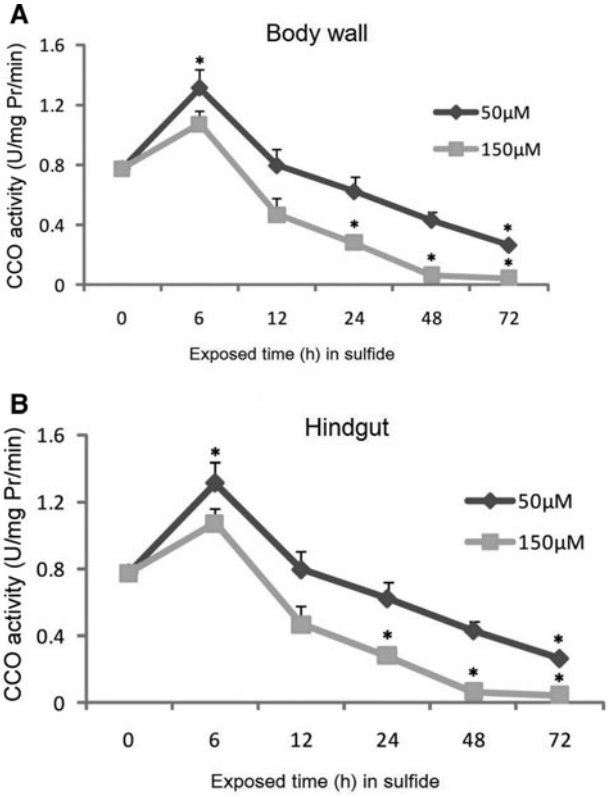

Fig. 5. CCO activity in body wall (A) and hindgut (B) of *Urechis unicinctus* exposed to sulphide. Data represent the mean ± SE, $N = 4$ with twp replicates. *, indicates significant difference from the 0 h control, $P < 0.05$.

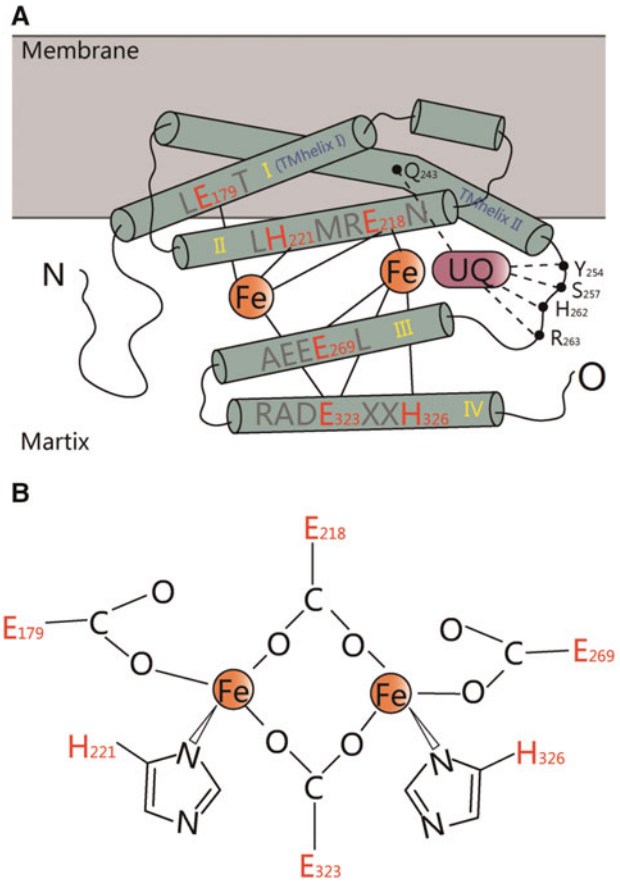

Fig. 6. Schematic structure of *Urechis unicinctus* AOX based on a model proposed by Andersson and Nordlund (modification from Berthold *et al.*, 2000): (A) the modified AN model. Cylinders with yellow Roman numerals represent the four-helix bundle in which the red letters represent conserved residues acting as iron-binding ligands (iron atoms are shown as red spheres). Cylinders with blue letters indicate transmembrane helices predicted by TMHMM. Black dots signify residues for quinine binding and UQ in pink represents the ubiquinone; (B) ligands of the di-iron centre in the modified AN model. See online publication for colour figure, doi: 10.1017/S0025315413000696

will disrupt the electron flow, increasing the cellular NADH/NAD+ ratio and placing the cell under reductive stress (Truong *et al.*, 2006). In addition, the inhibition of CCO will lead to incomplete oxygen reduction to water. All of these factors can increase the formation of ROS, which has the potential to disturb the homeostasis of the intracellular redox state, which is crucial for the correct functioning of most biological processes.

In the lugworm *Arenicola marina*, electrons from sulphide oxidation at lower sulphide levels can be passed to oxygen via the classical CCO pathway and coupled to ATP production. However, activity of CCO was blocked when sulphide concentrations were higher than 10 μM. The electrons from sulphide oxidation are thought to be transferred to oxygen via AOX (Völkel & Grieshaber, 1996). In our study, the activity of CCO decreased significantly at 24 h and was approximately zero at 48 h after 150 μM sulphide exposure, but significantly declined at 72 h after 50 μM sulphide exposure. Our results might imply that CCO of *U. unicinctus* has a greater tolerance to sulphide than *A. marina*. The mRNA expression of *U. unicinctus* AOX increased significantly at 48 h after sulphide exposure suggesting *U. unicinctus* AOX promoted the transfer of electrons from sulphide oxidation to oxygen, and thus decreased tissue damage in the worm caused by excess ROS production when CCO activity was inhibited. Our data experimentally support the hypothesis that an alternative sulphide oxidation pathway exists in animals and indicates a relevant role for AOX in establishing a protective mechanism against sulphide stress.

FINANCIAL SUPPORT

This work was supported by the Natural Science Foundation of China (NSFC) [40776074 and 31072191].

REFERENCES

Abramson J., Riistama S., Larsson G., Jasaitis A., Svensson-Ek M., Laakkonen L., Puustinen A., Iwata S. and Wikstrom M. (2000) The structure of the ubiquinol oxidase from *Escherichia coli* and its ubiquinone binding site. *Nature Structural and Molecular Biology* 7, 910–917.

Affonso E.G. and Rantin F.T. (2005) Respiratory responses of the air-breathing fish *Hoplosternum littorale* to hypoxia and hydrogen sulfide. *Comparative Biochemistry and Physiology* 141C, 275–280.

Affonso E.G., Polez V.L., Correa C.F., Mazon A.F., Araujo M.R., Moraes G. and Rantin F.T. (2004) Physiological responses to sulfide toxicity by the air-breathing catfish, *Hoplosternum littorale* (Siluriformes, Callichthyidae). *Comparative Biochemistry and Physiology* 139C, 251–257.

Affourtit C., Albury M.S., Crichton P.G. and Moore A.L. (2002) Exploring the molecular nature of alternative oxidase regulation and catalysis. *FEBS Letters* 510, 121–126.

Albury M.S., Affourtit C., Crichton P.G. and Moore A.L. (2002) Structure of the plant alternative oxidase. Site-directed mutagenesis provides new information on the active site and membrane topology. *Journal of Biological Chemistry* 277, 1190–1194.

Albury M.S., Elliott C. and Moore A.L. (2010) Ubiquinol-binding site in the alternative oxidase: mutagenesis reveals features important for substrate binding and inhibition. *Biochimica et Biophysica Acta (BBA)—Bioenergetics* 1797, 1933–1939.

Attene-Ramos M.S., Wagner E.D., Gaskins H.R. and Plewa M.J. (2007) Hydrogen sulfide induces direct radical-associated DNA damage. *Molecular Cancer Research* 5, 455–459.

Bagarinao T. (1992) Sulfide as an environmental factor and toxicant: tolerance and adaptations in aquatic organisms. *Aquatic Toxicology* 24, 21–62.

Bailly X. and Vinogradov S. (2005) The sulfide binding function of annelid hemoglobins: relic of an old biosystem? *Journal of Inorganic Biochemistry* 99, 142–150.

Berthold D.A., Andersson M.E. and Nordlund P. (2000) New insight into the structure and function of the alternative oxidase. *Biochimica et Biophysica Acta (BBA)—Bioenergetics* 1460, 241–254.

Berthold D.A., Voevodskaya N., Stenmark P., Graslund A. and Nordlund P. (2002) EPR studies of the mitochondrial alternative oxidase. Evidence for a diiron carboxylate center. *Journal of Biological Chemistry* 277, 43608–43614.

Buchner T., Abele D. and Pörtner H.O. (2001) Oxyconformity in the intertidal worm *Sipunculus nudus*: the mitochondrial background and energetic consequences. *Comparative Biochemistry and Physiology* 129B, 109–120.

Cooper C. and Brown G. (2008) The inhibition of mitochondrial cytochrome oxidase by the gases carbon monoxide, nitric oxide, hydrogen cyanide and hydrogen sulfide: chemical mechanism and physiological significance. *Journal of Bioenergetics and Biomembranes* 40, 533–539.

Eghbal M.A., Pennefather P.S. and O'Brien P.J. (2004) H_2S cytotoxicity mechanism involves reactive oxygen species formation and mitochondrial depolarisation. *Toxicology* 203, 69–76.

Fernandez-Ayala D.J., Sanz A., Vartiainen S., Kemppainen K.K., Babusiak M., Mustalahti E., Costa R., Tuomela T., Zeviani M., Chung J., O'Dell K.M., Rustin P. and Jacobs H.T. (2009) Expression of the *Ciona intestinalis* alternative oxidase (AOX) in *Drosophila* complements defects in mitochondrial oxidative phosphorylation. *Cell Metabolism* 9, 449–460.

Grieshaber M.K. and Völkel S. (1998) Animal adaptations for tolerance and exploitation of poisonous sulfide. *Annual Review of Physiology* 60, 33–53.

Goffredi S.K., Childress J.J., Desaulniers N.T., Lallier F.J. (1997) Sulfide acquisition by the vent worm *Riftia pachyptila* appears to be via uptake of HS^-, rather than H_2S. *Journal of Experimental Biology* 200, 2609–2616.

Gomes C.M., Le Gall J., Xavier A.V. and Teixeira M. (2001) Could a diiron-containing four-helix-bundle protein have been a primitive oxygen reductase? *ChemBioChem* 2, 583–587.

Hakkaart G.A., Dassa E.P., Jacobs H.T. and Rustin P. (2006) Allotopic expression of a mitochondrial alternative oxidase confers cyanide resistance to human cell respiration. *EMBO Reports* 7, 341–345.

Hand S.C. and Somero G.N. (1983) Energy metabolism pathways of hydrothermal vent animals: adaptations to a food-rich and sulfide-rich deep-sea environment. *Biological Bulletin. Marine Biological Laboratory, Woods Hole* 165, 167–181.

Hildebrandt T.M. and Grieshaber M.K. (2008a) Redox regulation of mitochondrial sulfide oxidation in the lugworm, *Arenicola marina*. *Journal of Experimental Biology* 211, 2617–2623.

Hildebrandt T.M. and Grieshaber M.K. (2008b) Three enzymatic activities catalyze the oxidation of sulfide to thiosulfate in mammalian and invertebrate mitochondria. *FEBS Journal* 275, 3352–3361.

Joyner-Matos J., Predmore B.L., Stein J.R., Leeuwenburgh C. and Julian D. (2010) Hydrogen sulfide induces oxidative damage to RNA and DNA in a sulfide-tolerant marine invertebrate. *Physiological and Biochemical Zoology* 83, 356–365.

Julian D., Wieting S.L., Seto S.L., Bogan M.R. and Arp A.J. (1999) Thiosulfate elimination and permeability in a sulfide-adapted marine invertebrate. *Physiological and Biochemical Zoology* 72, 416–425.

Kabil O. and Banerjee R. (2010) Redox biochemistry of hydrogen sulfide. *Journal of Biological Chemistry* 285, 21903–21907.

Kraus D., Doeller J. and Powell C. (1996) Sulfide may directly modify cytoplasmic hemoglobin deoxygenation in *Solemya reidi* gills. *Journal of Experimental Biology* 199, 1343–1352.

Ma Y.B., Zhang Z.F., Shao M.Y., Kang K.H., Tan Z. and Li J.L. (2010) Sulfide:quinone oxidoreductase from echiuran worm *Urechis unicinctus*. *Marine Biotechnology* 13, 1–15.

Maréchal A., Kido Y., Kita K., Moore A.L. and Rich P.R. (2009) Three redox states of *Trypanosoma brucei* alternative oxidase identified by infrared spectroscopy and electrochemistry. *Journal of Biological Chemistry* 284, 31827–31833.

McDonald A.E., Vanlerberghe G. and Staples J.F. (2009) Alternative oxidase in animals: unique characteristics and taxonomic distribution. *Journal of Experimental Biology* 212, 2627–2634.

Millero F.J., Plese T. and Fernandez M. (1988) The dissociation of hydrogen sulfide in seawater. *Limnology and Oceanography* 33, 69–74.

Moore A.L. and Albury M.S. (2008) Further insights into the structure of the alternative oxidase: from plants to parasites. *Biochemical Society Transactions* 036, 1022–1026.

Moore A.L., Carre J.E., Affourtit C., Albury M.S., Crichton P.G., Kita K. and Heathcote P. (2008) Compelling EPR evidence that the alternative oxidase is a diiron carboxylate protein. *Biochimica et Biophysica Acta* 1777, 327–330.

Muller M., Mentel M., van Hellemond J.J., Henze K., Woehle C., Gould S.B., Yu R.Y., van der Giezen M., Tielens A.G.M., Martin W.F. (2012). Biochemistry and evolution of anaerobic energy metabolism in eukaryotes. *Microbiology and Molecular Biology Reviews* 76, 444–495.

Nicholls P. (1975) The effect of sulfide on cytochrome aa_3. Isosteric and allosteric shifts of the reduced α-peak. *Biochimica et Biophysica Acta* 396, 24–35.

Oeschger R. and Storey K.B. (1990) Regulation of glycolytic enzymes in the marine invertebrate *Halicryptus spinulosus* (Priapulida) during environmental anoxia and exposure to hydrogen sulfide. *Marine Biology* 106, 261–266.

Pichaud N., Rioux P. and Blier P.U. (2012) *In situ* quantification of mitochondrial respiration in permeabilized fibers of a marine invertebrate with low aerobic capacity. *Comparative Biochemistry and Physiology* 161A, 429–35.

Powell M.A. and Somero G.N. (1986) Hydrogen sulfide oxidation is coupled to oxidative phosphorylation in mitochondria of *Solemya reidi*. *Science* 233, 563–566.

Schroff G. (1977) Anaerobic reduction of fumarate in the body wall musculature of *Arenicola marina* (Polychaeta). *Comparative Biochemistry and Physiology* 116B, 325–336.

Sluse F.E. and Jarmuszkiewicz W. (1998) Alternative oxidase in the branched mitochondrial respiratory network: an overview on

https://doi.org/10.1017/S0025315413000696 Published online by Cambridge University Press

structure, function, regulation, and role. *Brazilian Journal of Medical and Biological Research* 31, 733–747.

Taniguchi E., Matsunami M., Kimura T., Yonezawa D., Ishiki T., Sekiguchi F., Nishikawa H., Maeda Y., Ishikura H. and Kawabata A. (2009) Rhodanese, but not cystathionine-gamma-lyase, is associated with dextran sulfate sodium-evoked colitis in mice: a sign of impaired colonic sulfide detoxification? *Toxicology* 264, 96–103.

Theissen U. and Martin W. (2008) Sulfide: quinone oxidoreductase (SQR) from the lugworm *Arenicola marina* shows cyanide- and thioredoxin-dependent activity. *FEBS Journal* 275, 1131–1139.

Tiranti V., Viscomi C., Hildebrandt T., Di Meo I., Mineri R., Tiveron C.D., Levitt M., Prelle A., Fagiolari G., Rimoldi M. and Zeviani M. (2009) Loss of ETHE1, a mitochondrial dioxygenase, causes fatal sulfide toxicity in ethylmalonic encephalopathy. *Nature Medicine* 15, 200–205.

Truong D.H., Eghbal M.A., Hindmarsh W., Roth S.H. and O'Brien P.J. (2006) Molecular mechanisms of hydrogen sulfide toxicity. *Drug Metabolism Reviews* 38, 733–744.

Völkel S. and Grieshaber M.K. (1996) Mitochondrial sulfide oxidation in *Arenicola marina*: evidence for alternative electron pathways. *European Journal of Biochemistry* 235, 231–237.

and

Vanlerberghe G.C. and McIntosh L. (1997) Alternative oxidase: from gene to function. *Annual Review of Plant Physiology and Plant Molecular Biology* 48, 703–734.

Correspondence should be addressed to:
Z. Zhang
Key Laboratory of Marine Genetics and Breeding (Ocean University of China), Ministry of Education, Qingdao 266003, China
email: zzfp107@ouc.edu.cn.

https://doi.org/10.1017/S0025315413000696 Published online by Cambridge University Press